Carbohydrate Polymer Technologies and Applications 7 (2024) 100517

Contents lists available at ScienceDirect

Carbohydrate Polymer Technologies and Applications

journal homepage: www.sciencedirect.com/journal/carbohydrate-polymer-technologies-and-applications

Effect of bacterial cellulose on the foaming properties of egg white and soy proteins

Daniela Martins [a,b], Niloofar Khodamoradi [a], Ricardo Silva-Carvalho [a,b], Miguel Gama [a,b,*], Mehran Moradi [c], Fernando Dourado [a,b]

[a] CEB- Centre of Biological Engineering, Campus de Gualtar, Universidade do Minho, Braga 4710-057, Portugal
[b] LABBELS—Associate Laboratory, Braga 4710-057, Portugal
[c] Department of Food Hygiene and Quality Control, Faculty of Veterinary Medicine, Urmia University, Urmia 1177, Iran

ARTICLE INFO

Keywords:
Aqueous foams
Egg white protein
Soy protein
Bacterial cellulose

ABSTRACT

Food foams are highly industrially relevant systems, responsible for the visual appearance and organoleptic properties of many processed foods. Foam characteristics can be further improved by food-grade additives. This study investigates the influence of bacterial cellulose (BC) on the foaming capacity (FC) and foam stability (FS) of egg white protein (EWP) and soy protein isolate (SPI), important food foaming agents. The effects of pH, BC concentration and particle size on the FS and FC were analyzed. Compared to SPI, EWP demonstrated higher FC, an effect that is tentatively assigned to its lower molecular weight, hence faster diffusion to the interface. Adding 0.1 % BC to EWP (4 %, at pH 7.0) and to SPI (4 %, at pH 3.0) increased the FC by 1.6 and 1.5 times, respectively. The addition of BC also reduced the foam's liquid drainage, although not impacting the FS. Surprisingly, large flakes of BC ($D_v(50)$ of 1104 μm) yielded higher FC values than smaller ones. We hypothesize that larger BC flakes may act as anchoring sites, stabilizing the air bubbles during whipping. BC flakes were observed in the plateau borders and nodes of EWP foams, clogging the water channels and preventing drainage. This work demonstrates the potential of BC as a food-grade foam enhancer, providing a new tool for the food engineer's arsenal.

1. Introduction

Foams are two-phase systems that consist of a high volume of air cells (discontinuous phase) separated by a thin, continuous liquid layer (lamellar phase) (Zayas, 1997). In many processed foods, foams can provide a unique range of textures, as those seen in cake, bread, and confectionery products such as whipped cream, ice cream, mousse and soufflés. The uniformity of a foam enhances its taste and texture. However, producing and stabilizing a foam with a lot of gas bubbles can be challenging due to their tendency for relatively rapid creaming, dissolution and coalescence, film drainage, film rupture and disproportionation (Tang et al., 2022; Razi et al., 2022; Jin et al., 2023; Ma et al., 2022; Gao et al., 2022; Murray, 2020; Foegeding et al., 2006).

A good foaming agent should rapidly adhere to a hydrophilic-hydrophobic interface and form a robust interfacial film, decreasing its surface tension. Superior foaming performance means better product volume, structure, texture and stability (Tang et al., 2022; Jin et al., 2023; Ma et al., 2022; Gao et al., 2022). Proteins are widely used as foaming agents because they spontaneously adsorb onto air/water interfaces, decreasing the surface tension of the liquid phase and stabilizing the foam structure (Zayas, 1997; Murray, 2020; Foegeding et al., 2006; Narsimhan & Xiang, 2018; Zhang et al., 2022; Xiao et al., 2021; Wang et al., 2022; Zhang et al., 2022; Zhang et al., 2023; Jin et al., 2022; Jin et al., 2022; Sun et al., 2022). Egg white protein (EWP) still comprises the most widespread foaming agent among several. There has also been an increasing interest in substituting EWP with plant-based alternatives, such as soy protein isolate (SPI), to reduce the reliance on animal proteins. However, the surface activity and foaming capacity of SPI (and other plant-based proteins) are constrained by its rigid structure and poor solubility (Li et al., 2022; Warnakulasuriya & Nickerson, 2018). Some studies have shown that a pre-treatment of the proteins, a chemical or physical induced modification, can sometimes improve their foamability (He et al., 2015; Xia et al., 2022). In cases where the foaming agent alone is ineffective in creating and maintaining a strong pore structure, edible foams can benefit from the addition of a food-grade stabilizer. These stabilizers may further increase the surface

* Corresponding author at: Departamento de Engenharia Biológica, Universidade do Minho, Campus de Gualtar, Braga 4710-057, Portugal.
E-mail address: fmgama@deb.uminho.pt (M. Gama).

https://doi.org/10.1016/j.carpta.2024.100517

Available online 21 May 2024

hydrophobicity and reduce the surface tension, improve the viscoelasticity, prevent liquid drainage and film rupture, increasing stability. Among these stabilizers are sugars and polysaccharides, modified celluloses, peptides, microgel particles and others (Dabestani & Yeganehzad, 2019; Dickinson, 2017; Oduse et al., 2018; Dickinson, 2020).

Plant nano/micro cellulose have captured an increasing interest as colloid stabilizers in food formulations (Perumal et al., 2022) in particular for generating stable liquid-liquid emulsions through adsorption at the interface and by structuring the continuous phase (Bertsch et al., 2019). Foam systems stabilized by solid particles, including cellulose, have also been reported (Hu et al., 2016; Cervin et al., 2015; Capron et al., 2017). If particles are hydrophilic, they tend to accumulate in the plateau borders of foams, thereby slowing down the liquid drainage and kinetically increasing the foam stability (Alargova et al., 2004; Pugh, 1996). Particularly, the crystal faces of nano/micro cellulose may bear amphiphilic character and surface activity (Capron et al., 2017). While proper foaming requires the fast adsorption of the stabilizer at the air/liquid interface, the adsorption of nano/micro-sized particles is impaired by particle diffusion to the interface and a kinetic adsorption barrier near the interface (Kutuzov et al., 2007; Lam et al., 2014). Consequently, cellulose particles are not good foaming agents, unless they are subjected to surface modifications to alter their hydrophobicity, or adsorbed to charged, surface-active molecules (Hu et al., 2016; Cervin et al., 2015). However, they can improve the stability and mechanical properties of protein foams.

In addition to plants, several bacterial species synthesize cellulose nanofibrils known as bacterial cellulose (BC), which may be obtained with high purity. Also, the nanofibrillated structure of BC results in a huge surface area, enabling the absorption of nearly 200 times its mass in water. Due to its high water absorption and holding capacity, high crystallinity, high tensile strength, mechanical strength, high porosity and permeability to gas and liquid (Lee et al., 2014; Keshk, 2014; Andrade & Pertile, 2010; Navya et al., 2022), BC is an excellent platform for a variety of applications in several fields (Azeredo et al., 2019; de Amorim et al., 2020; Gregory et al., 2021; T. Li et al., 2021; Cazón & Vázquez, 2021). It exhibits amphiphilic characteristics that are essential for stabilizing air-liquid (foams) and liquid-liquid (emulsions) interfaces (Capron et al., 2017; Kalashnikova et al., 2012; Medronho & Lindman, 2014). BC is currently consumed as a food product, Nata de Coco, in various Asian countries. It has been proposed as a low-calorie bulking ingredient for the production of innovative, rich functional foods in various forms, thanks to its suspending, thickening, water-retaining, stabilizing, bulking and fluid qualities (Perumal et al., 2022; Andrade & Pertile, 2010; Q. Li et al., 2021; Shi et al., 2014).

As above-mentioned, the effect of plant- and wood-derived cellulose on the stabilization of interfaces, particularly liquid-air interfaces in foams, is documented. It has also been demonstrated that BC nanofibers alone have interface stabilizing characteristics in oil/water systems (Martins et al., 2020) and can also improve the emulsifying capacity of proteins, as has been reported for e.g. soy protein isolate in high internal-phase Pickering emulsions (Liu et al., 2021) and for whey protein isolate in olive oil-in-water emulsions (Paximada et al., 2016). BC fibers also have a higher aspect ratio than their plant-derived counterpart, which has been shown to be beneficial for the stabilization of both emulsions and foams (Capron et al., 2017; Kalashnikova et al., 2011; Kondo et al., 2016). However, to the authors' knowledge, the use of BC in the development of aqueous food foams is scarce. The few publications somehow related to the use of BC in edible foams include a report by Okiyama et al. (1993) where 0.5 % BC pulp added to ice cream prevented its meltdown and stabilized its shape for 1 h, and by Zhang et al. (2020) who produced edible solid foams by freeze-drying an oil-in-water emulsion stabilized by BC and SPI. In this study, we examine, for the first time, the effect of BC on the capacity and stability of EWP and SPI aqueous foams, describe the effect of BC on the foaming properties of these proteins, and finally propose a novel application for BC in the food industry.

2. Materials and methods

2.1. Materials

BC wet membranes (a food product commonly known as *Nata de coco*) were supplied by HTK Food Co., Ltd. (Ho Chi Minh, Vietnam), and their detailed characterization can be found in Queirós et al. (2021). Egg white protein powder (EWP, 84 % protein) was acquired from a local market in Portugal. Vegacon 90 LV soy protein isolate (SPI, minimum 90 % protein) was obtained from Eurosoy GmbH (Hamburg, Germany). Avicel® colloidal MCCs were supplied by DuPont (Wilmington, Delaware, USA). CelluForce NCC, was supplied by Celluforce Inc, USA. Calcofluor and Rhodamine B were obtained from Sigma (St. Louis, Missouri, USA). Hydrochloric acid (HCl) was purchased from Fisher-Chemical (Loughborough, U. K.), and sodium hydroxide (NaOH) from Labkem (Barcelona, Spain).

2.2. Preparation of BC

BC membranes were prepared as described elsewhere (Martins et al., 2020). Briefly, BC membranes were submerged in a 0.1 M NaOH aqueous solution, at room temperature, for two days (with daily exchange of the solution) and then submerged in distilled water, also with daily exchanges, until the pH of the washing water was constant and matched that of the clean distilled water. The membranes were then ground with a Sammic TR250 (Sammic S. L.) hand blender, at 9000 rpm for about 1 to 2 min, until a homogenous pulp was obtained (BC), as observed by visual inspection (absence of visible unfragmented membrane pieces). This mixture was stored at 4 ºC until use. A portion of the hand-blended BC pulp was further processed in a high-speed blender (Moulinex Ultrablend 1500 W, Écully, France) at 24,000 rpm for 30 min (in 5 min intervals to prevent overheating) - designated HSB-BC. Another sample of the hand-blended BC was further processed in a High-Pressure Homogenizer (GEA Niro Soavi, model Panther NS3006L), for two cycles at 600 Bar – designated HPH-BC. The solid fraction of all BC pulps was determined by dry weight and adjusted to 0.8 % (m/m). Characterization of the particle size of the ground BC pulps was done as described ahead (Section 2.3).

2.3. Characterization of the particle size of BC

The size distribution of the flakes in the BC pulps, processed as described above, was determined as described by Martins et al. (2020), using a Malvern Mastersizer 3000 laser diffraction instrument equipped with a Hydro EV sample dispersion unit (Malvern Panalytical, Malvern, UK). Briefly, aqueous suspensions of BC, HSB-BC, or HPH-BC samples were added to the dispersion unit prefilled with tap water, until an obscuration level between 10 and 20 % was reached. The stirring rate in the dispersion unit was set at 1500 rpm with initial ultrasonication (35 W) for 10 s. The detector array measured the scattering pattern for 30 s. Five measurements were performed per sample. The refractive index of BC and water were assumed as 1.468 and 1.330 respectively (as provided by the software's database) and Mie scattering model for non-spherical particles was used. The particle size was then expressed as the volume distribution percentiles, Dv(10), Dv(50), and Dv(90); also, the Volume Moment Mean, $D_{[4,3]}$, and the Surface Area Mean, $D_{[3,2]}$ were recorded.

2.4. Zeta potential of protein solutions

To measure the zeta potential of the protein solutions at different pH, EWP or SPI were dissolved in distilled water at a concentration of 0.05 %, and the pH was adjusted within the range of 2.0 to 8.0 with 6 M HCl or 10 M NaOH, as needed. All samples were analyzed three times using a Zetasizer Nano ZS (Malvern Instruments Ltd.) with disposable folded capillary cells.

2.5. Surface tension of protein solutions and cellulose dispersions

EWP and SPI solutions were prepared at 4 % in distilled water, at room temperature, with magnetic stirring (200 rpm) for 2 h. The pH of the protein solutions was kept at 7.0 or adjusted to 3.0 with HCl 6 M. Considering the technical challenges in determining the surface activity of BC suspensions, other celluloses featuring low particle sizes were used to characterize their effect on surface tension. Celluforce NCC (cellulose nanocrystals) was dispersed in distilled water to a concentration of 0.5 % (w/w) and stirred for 20 min. Avicel was also dispersed in distilled water to a concentration of 2 % and then activated using high-shear mixing at 20,000 rpm for 20 min (as instructed by the manufacturer) in a digital T-25 Ultra-turrax with a dispersing tool (IKA, Germany) and then diluted to 0.5 %. All prepared samples were stored at 4 ºC before use. The surface tension of the samples was quantified through the pendant drop method, using an Optical Contact Angle device (OCA 20; DataPhysics) and SCA 20 Software Module 22 (DataPhysics) (Song & Springer, 1996). Samples were left at rest for a few minutes to reach thermal equilibrium (20 ºC). Each sample was then transferred to a B. Braun 1 mL disposable syringe with a blunt tip needle of 0.71 mm outer diameter and placed in the OCA device. To produce stable drops, the maximum drop volume was first determined for each sample; then, drops were made at the maximum volume for the analysis. The software automatically determined the surface tension based on the drop's profile, 10 times per minute until 25 readings were acquired per sample. The surface tension value for each sample was calculated as the average of the 25 readings. Assays were done in triplicate.

2.6. Foams generation

First, protein solutions were prepared (100 mL final volume) by dissolving EWP or SPI powders in distilled water to reach a final protein content of 4 % or 12 %, and stirred for 2 h at 200 rpm and room temperature. The selected concentrations in this study correspond to the protein content found in raw eggs (12 %) (Tang et al., 2021) and to the optimized concentration for producing foam from SPI, as described in Grimaldez & Martínez (2021) (Sullca Grimaldez & Martínez, 2021). The concentration of soluble protein obtained for a content of 4 %, at pH 3.0 and 7.0, was determined with the Pierce BCA Protein Assay kit, using Bovine Serum Albumin as standard. After dispersion of the proteins as above described, the mixture was centrifuged at 2000 rpm for 10 min (Centrifuge 5430 R, Eppendorf) at 25 °C, and the protein was determined on samples collected before and after centrifugation.

Protein foams were prepared using a Kitchen Aid Ultra Power Mixer (Kitchen Aid, St. Joseph, MI) with a 4.3 L stationary bowl and revolving beaters. To prepare the control foams, protein solutions were beaten at maximum speed for a total of 5 min. Immediately after whipping, each foam was carefully transferred to a measuring beaker using a rubber spatula, eliminating any voids and enabling a homogeneous distribution of the foam inside the beaker. All foams were kept undisturbed at room temperature during the stability analysis.

2.6.1. Effect of BC concentration and size

To produce foams with protein and BC, EWP or SPI powders were dissolved in distilled water (2 h, 200 rpm), discounting the volume of water to be added from the BC pulp. Then, the 0.8 % BC pulp was added to the protein solutions: 12.5 g, 37.5 g or 62.5 g of pulp, to reach the final BC concentrations of 0.1 %, 0.3 %, or 0.5 % (m/m) respectively, before starting the whipping process. After adding BC, the mixture was whipped at maximum speed for 5 min. The same procedure was applied for HSB-BC and HPH-BC pulps to obtain a final concentration of 0.1 %. After whipping, test foams were individually transferred to measuring beakers and handled as described for control foams in Section 2.6.

2.7. Determination of foam capacity (FC) and foam stability (FS)

Protein foaming capacity (FC) is the ability of a continuous phase to incorporate air when whipped, measured by the increase in volume. Protein foam stability (FS) is the ability to retain air over time, measured by the percentage change in foam volume over time (Ding et al., 2020). Foam stability can also be described by the volume of liquid (continuous phase) that drains from the foam to the bottom of the container, reducing the thickness of the liquid films separating the air pockets. The volume of the foam and of the drained liquid (DL) were recorded over time, and the FC and FS of samples were calculated using the following equations:

$$FC(\%) = \frac{V_1}{V_0} \times 100 \quad (1)$$

$$FS(\%) = \frac{(V_t - DL_t)}{V_1} \times 100 \quad (2)$$

where V_0 was the initial liquid sample volume (before whipping, 100 mL), V_1 is the foam volume immediately after whipping, V_t is the foam volume at each storage timepoint and DL_t stands for the drained liquid at each timepoint. All experiments were done in triplicate and the mean results and standard deviations were calculated.

2.8. Effect of pH on the FC and FS

To investigate how pH affects the FC and FS of the protein's liquid foams (and their mixtures with BC), the pH of the protein solutions (SPI and EWP) in distilled water was first measured at room temperature and found to be approximately 7.0 at all tested concentrations. To produce foams, before whipping (as above in 2.4), the protein solutions were either used without treatment (pH ~ 7.0) or adjusted to pH 3.0 with 6 M HCl.

2.9. Microscopic observations

For bright field optical microscopy, foams were prepared as described in Section 2.4, placed in a glass slide, and observed in an Olympus BX51 fluorescence microscope (Olympus Europa SE & Co. KG, Hamburg, Germany), in bright field, with a 10x magnification objective lens. Bubbles' diameter in the obtained pictures was measured using the Fiji ImageJ software (NIH). A minimum of 400 bubbles were measured per sample.

For a better understanding of the foam structure and BC distribution in the continuous phase, before whipping, the protein solutions at 4 % were stained with 1 mL of rhodamine B solution (0.1 mg/mL in water) and the BC pulp with 1 mL of Calcofluor White stain solution (0.05 mg/mL in distilled water). Stained foam samples were prepared protected from light. The prepared foam samples were then placed in glass slides and observed using an Olympus BX51 fluorescence microscope with a DAPI filter (excitation wavelength: 360–370 nm; emission wavelength: 420 nm) and a TRITC filter (excitation: 530–550 nm; emission: 590 nm).

2.10. Rheological analysis of foams

Rheological measurements of the foams were made immediately after they were prepared, using a hybrid rheometer (DHR-1, TA instruments) with TRIOS Software (TA Instruments). Measurements were made at 20 °C using a 40 mm diameter stainless steel plate geometry. Due to the heterogeneity of the foams, a 2 mm gap was determined to be the most appropriate condition for the assays. To analyze the viscoelastic properties of the foams (complex viscosity and viscoelastic moduli G' and G''), oscillatory strain Sweep tests were first performed between 0.02 and 100 % strain at a frequency of 1 Hz to determine the linear viscoelastic region (LVR). Then, frequency sweep tests were run in

the range of 0.1 to 20 Hz, at 0.5 % strain (within the LVR of all samples). The average and standard deviation of the analysis of triplicate samples were plotted.

2.11. Statistical analysis

All data generated in this study was analyzed by GraphPad Prism 9 for Windows, GraphPad Software, San Diego, California, USA. Within each group, a one-way ANOVA (Analysis of Variance) with Tukey's multiple comparisons test (95 % confidence) was used to compare the mean values. To compare the means between groups, a two-way ANOVA, with Šídák's multiple comparisons test was used.

3. Results and discussion

3.1. Surface tension and zeta potential

The whipping process, generating bubbles and foaming, increases the surface area and thus the surface energy, introducing structural instability. A transient stability can be achieved by using surface active agents, such as proteins, that lower the surface tension of the liquid film (Butt et al., 2003). Fig. 1 shows that, regardless of the pH, both EWP and SPI reduce ($p < 0.05$) the water surface tension to around 40–50 mN/m. Surprisingly, given the well-known superior foaming ability of EWP over other proteins (Jin et al., 2023; Murray, 2020; Foegeding et al., 2006), SPI showed a slightly higher reduction of the surface tension, especially at pH 7.0. This apparent contradiction can be explained when considering the size of the proteins. SPI consists of two major proteins, glycinin, with a molecular weight of 340–375 kDa and β-conglycinin, with a molecular weight of 140–170 kDa (Luo et al., 2017; Urade, 2011). On the other hand, ovalbumin (54 %) with a molecular weight of 45 kDa and ovotransferrin (12 %) with a molecular weight of 76 kDa, are the major proteins found in EWP (Abeyrathne et al., 2013). Thus, the higher ability of EWP to incorporate air, as compared to SPI and other plant-based proteins, may be explained by the higher diffusion rate and adsorption at the interface of water-air bubbles (Delahaije et al., 2014), given their lower overall molecular weight. Consequently, proteins in EWP may stabilize air bubbles faster, during whipping. This effect may also be justified by the higher solubility of EWP. As shown on Table 1, centrifugation removed just a relatively small portion of the EWP at both pH values (the soluble fraction is not far from the total protein quantified in the initial samples), while a substantial amount was removed in the case of SPI. A value close to the expected 4 % (40 mg/mL) was obtained for EWP, confirming its good solubility, while a much lower value was determined for SPI, probably because, being partially aggregated/insoluble, the protein was only partially quantified using the colorimetric BCA method. This result is not unexpected, since SPI is known for its poor solubility, as remarked in the introduction.

Table 1
EWP and SPI concentration (mg/mL) at pH 3.0 and 7.0, measured before (Total) and after centrifugation (Soluble).

	EWP		SPI	
pH	3.0	7.0	3.0	7.0
Total (mg/mL)	42.14 ± 1.47	43.36 ± 2.41	21.86 ± 0.54	27.15 ± 1.85
Soluble (mg/mL)	37.46 ± 1.57	36.60 ± 1.34	11.06 ± 0.52	12.83 ± 0.50

We could not measure the effect of BC ground with the hand-blender on the surface tension, since it got stuck in the syringe of the pendant-drop surface tension meter due to the large size of the flakes, resulting in artifacts. However, we were able to use HPH-BC and other plant-based celluloses with small particle sizes. Regarding Avicel particles, they were treated with a high-shear homogenizer, as instructed by the manufacturer, until they ceased to sediment. As shown in Fig. 1, the surface tension of the water-air system does not vary significantly ($p > 0.05$) with any of the studied celluloses: microcrystalline (Avicel), nanocrystalline (Celluforce), or nanofibrillar (HPH-BC). Thus, any changes in the FC with the addition of cellulose cannot be directly related to an effect on surface tension.

The pH may have a significant effect on protein liquid foams, as it is the main driver of the protein charge. In turn, this affects intermolecular interactions, particularly those between proteins adsorbed on both sides of the lamellae film (Butt et al., 2003; Butt et al., 2003; Barnes & Gentle, 2011). Charged proteins tend to repel each other, increasing the disjoining pressure and consequently reducing capillary pressure, giving rise to better foaming capacity and a more stable foam (Narsimhan & Xiang, 2018; Butt et al., 2003; Barnes & Gentle, 2011; Engelhardt et al., 2013; Mohanan et al., 2020; Kuropatwa et al., 2009).

The zeta potential of EWP and SPI, as a function of pH, is shown in Fig. 2. It may be observed that both proteins are positively and negatively charged, respectively, at pH 3.0 and 7.0. However, EWP presents higher zeta potential values (less negative) than SPI at pH above 5. Thus,

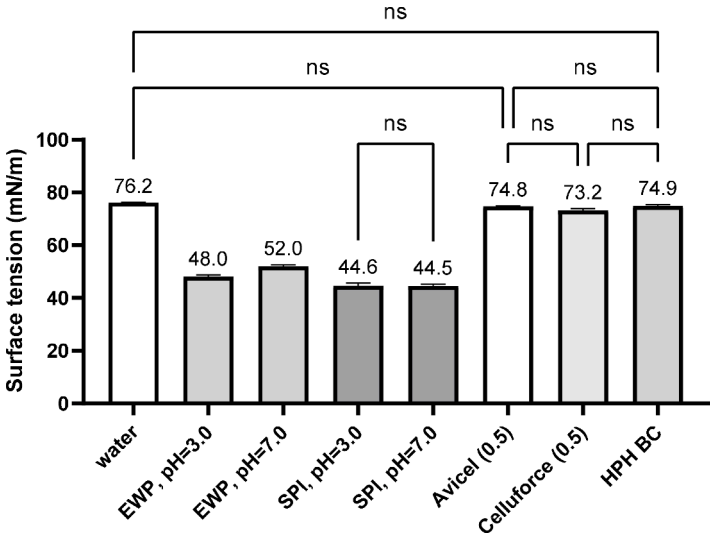

Fig. 1. Surface tension values of water, egg white protein (EWP) and soy protein isolate (SPI) solutions at 4 % and at different pH, and of aqueous dispersions of homogenized bacterial cellulose (HPH-BC) and plant celluloses (i.e., Avicel and Celluforce) at 0.5 %. For the sake of clarity, only non-significant differences (ns, $p > 0.05$) are identified.

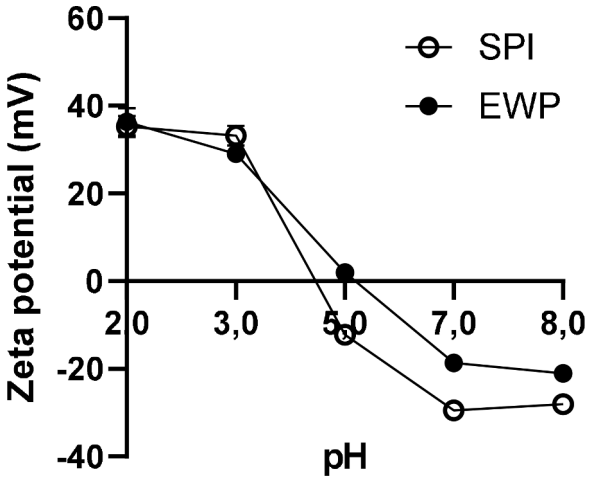

Fig. 2. Zeta potential of EWP and SPI solutions, at 0.05 % concentration, as a function of pH.

SPI could be expected to generate a higher disjoining pressure than EWP, although a more definitive assessment would require the estimation of the protein concentration at the interface (which may be affected by the rate of diffusion).

3.2. Optimization of BC concentration and particle size on EWP foams

As shown in Fig. 3, a small amount of BC (0.1 %) increases by 1.4 times the FC of 12 % EWP solutions (as compared to the control), but this effect is lost if a higher amount of BC (0.3 %) is added, as the FC decreases to values closer to the control group. Thus, for 12 % EWP, the effect of the BC concentration goes through an optimal value. In contrast, an insignificant effect of BC on the FS was observed ($p > 0.05$), which remained high for up to 2 h of storage, irrespective of the added BC concentration. However, despite the relatively constant foam volume, a reduction in the (very high) amount of drained liquid was evidenced in foams containing BC; in this case, an increase in BC concentration led to a higher reduction of the drained liquid. While the control protein foams became dry and fragile during storage, BC-containing foams were able to better retain the liquid in the continuous phase. Similar results were obtained for 4 % EWP foams (Fig. 3B), where the FC increased from 700 to over 1100 % upon incorporating BC at a concentration of 0.1 to 0.3 % (a 1.6-fold increase); again, when further increasing the BC concentration to 0.5 %, this effect was lost and the FC decreased to values below the control. Also in this case (4 % EWP), the FS showed minimal changes over time, but the drained liquid exhibited an inverse proportionality to the BC concentration (as was seen for 12 % EWP). Consequently, BC at a concentration of 0.1 % was selected for further studies, as it gives the optimal FC in both EWP concentrations studied.

Literature shows that as protein concentration rises, the rate of protein adsorption at the air–water interface accelerates, resulting in a decrease in surface tension and, consequently, an increase in foaming capacity. Also, the formation of a multilayer of globular proteins (as is the case of EWP) increases with protein concentration and provides stability to the foams (Indrawati et al., 2008). This suggests that, at higher protein concentration, the FS would be higher. However, both the FC and FS of 4 % and 12 % EWP were similar ($p > 0.05$). The foaming properties of EWP had possibly reached a saturation point at 4 % due to limitations in the available air–water interface or the structure of the protein layer. On the other hand, interestingly, the effect of BC is slightly

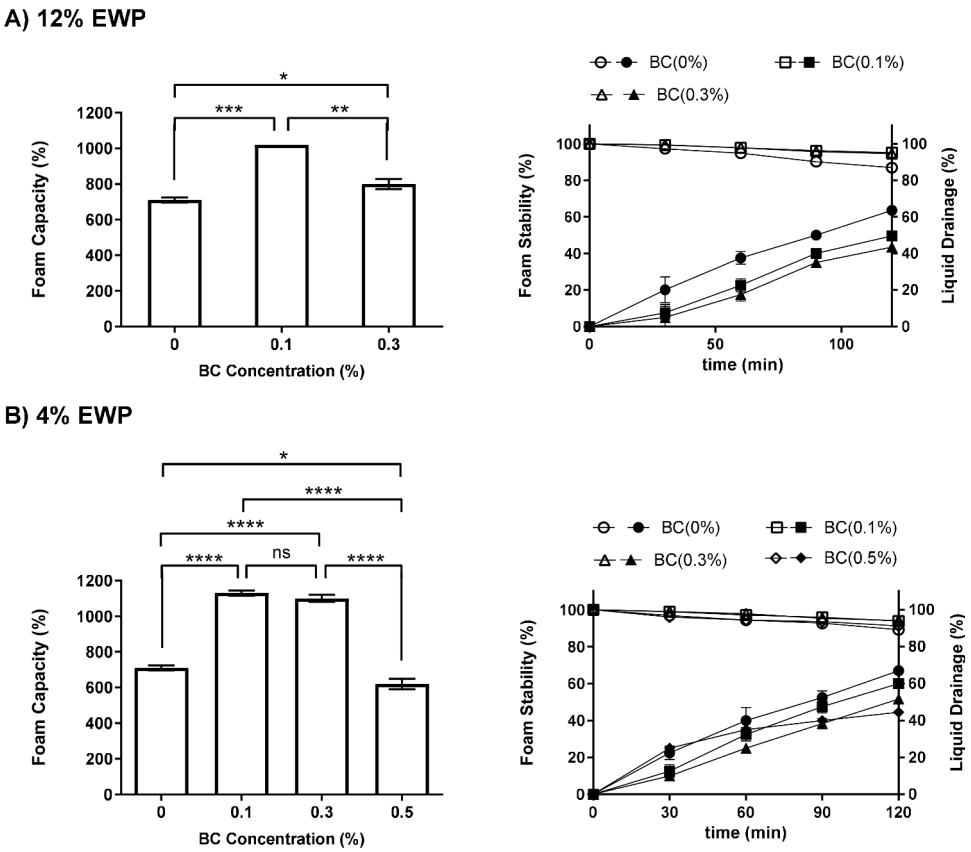

Fig. 3. Left side: foaming capacity; right side: foam stability (hollow symbols) and liquid drainage (full symbols) of **A**) 12 % egg white protein (EWP) and **B**) 4 % EWP, with different concentrations of bacterial cellulose (BC) at pH 7.0. Datasets were compared with each other using one-way ANOVA followed by Tukey's Multiple Comparison Test (significant statistical differences at * $p < 0.05$, ** $p < 0.01$, *** $p < 0.001$, **** $p < 0.0001$; ns - not significant).

superior and observed for a larger range of concentration for the 4 % EWP dispersion.

We investigated the effect of further BC comminution (in a high-speed blender and in a high-pressure homogenizer) on the particle size and the subsequent effect on the foams' properties. Table 2 shows the mean particle size and size distributions, as measured by Mastersizer analysis.

Upon initial mechanical shear (high-speed blending) of the hand-blended BC, the 3D fiber network was fragmented into fiber flakes or bundles of variable size and shape. These flakes have a star-like structure, wherein loose fiber branches emerge from a deeply entangled core (Martins et al., 2020). As shown by the volume distribution values in Table 2, the size of the flakes decreases with increasing grinding time and shear, from short-time hand blender fragmentation to longer contact time with high-speed blades (HSB) or high-pressure homogenization (HPH).

As shown in Fig. 4, only the bigger BC flakes from low-speed hand-blending resulted in a higher EWP (4 %, at pH 7.0) foam capacity, whereas the smaller ones from HSB and HPH BC had no effect, being similar ($p > 0.05$) to a control (without BC). Foam stability was similar across all conditions. This surprising result shows that larger flakes of BC are required to achieve the capacity-boosting effect observed. This is paradoxical, as it could be expected that smaller fibers could more effectively conform to the narrow plateau borders and their convergence nodes. While the size of BC flakes seems to be functionally important to improve FC, this seems not to rely on the reduction in surface tension, as shown in Fig. 1.

These optimized parameters can have direct and positive implications in the formulation of certain food products. The addition of shortly processed BC in low concentrations allows for an increase in the volume of incorporated air in the foam (higher FC), which is desirable for obtaining food products with a light and airy texture, such as batters, ice creams and mousses. The total volume of the foam remains practically constant for up to 2 h, but more importantly, the water is retained in the matrix for longer (slower drainage), preventing drying of the foam and changes in its consistency (important, for example, in meringue and whipped cream).

3.3. Effect of BC and pH on EWP and SPI foams

After studying the effect of BC characteristics on EWP foams, SPI was included in this study since it is a relevant non-animal source of protein in food technology, and to ascertain whether the observed effect of BC in EWP foams also occurs with proteins from different sources. However, SPI could not be adequately dispersed at very high concentrations, such as 12 %, and it has already been reported that 4 % is the optimal concentration for producing SPI foams (Sullca Grimaldez & Martínez, 2021). Thus, although SPI is not fully soluble at 4 % (Table 1), since this concentration also showed better FC results for EWP, it was chosen for further analysis with both proteins.

The effect of pH on the FC and FS of EWP and SPI foams, with or without 0.1 % BC, is illustrated in Fig. 5. In general, EWP exhibits greater FS than SPI. As discussed above, the superior foaming capacity of EWP may be assigned, at least partially, to its lower molecular weight and better solubility. Surprisingly, while BC did not improve ($p > 0.05$) the FC of SPI at neutral pH (as observed for EWP, Fig. 5A), it had a more pronounced effect at pH 3.0, increasing the SPI foam capacity by 1.5 fold (Fig. 5B), approaching that of EWP at pH 7.0. Thus, BC had a more significant effect on the FC of EWP at pH 7.0 and of SPI at pH 3.0. Interestingly, BC appears to improve the FC at a pH more favorable for each protein to develop foam (without BC, pH 7.0 is slightly preferable for EWP and pH 3.0 for SPI). With regards to the FS of EWP foams, within a 3 h timeframe, regardless of the pH, BC had no effect. Conversely, a more significant effect of BC was observed for SPI foams, which were much less stable than EWP foams. At pH 3.0, BC supported the FS for a few hours, as compared to the control, whereas at pH 7.0 it had no effect. Nevertheless, from this study, a more remarkable effect of BC seems to be related to the significant increase in the FC of proteins.

The values of surface tension and protein charge, comparable for the two proteins, don't provide any obvious justification for the observed difference in the foam stability values (superior in the case of EWP – most likely due to the lower molecular weight), and do not explain why BC improves the FC at different pH values for each protein. We speculate that different structural conformations of SPI and EWP at the two tested pH, allowing more favorable (e.g., hydrophobic) interactions at the more favorable pH for each protein (3 for SPI and 7 for EWP), may justify the obtained results.

Table 2
Size distribution (by volume) percentiles and mean diameters of BC samples ground by different methods*.

	Percentiles (μm)			Mean diameters (μm)	
BC samples	$D_v(10)$	$D_v(50)$	$D_v(90)$	$D_{[3,2]}$	$D_{[4,3]}$
BC	254 ± 100	1104 ± 161	2299 ± 165	514 ± 137	1205 ± 140
HSB-BC	13 ± 1	52 ± 4	139 ± 3	29 ± 2	65 ± 2
HPH-BC	24 ± 1	71 ± 2	187 ± 8	50 ± 2	91 ± 4

* BC: obtained using a hand-blender; HSB: high-speed blender; HPH: high pressure homogenizer, 2 passages.

3.4. Microscopical observation of foams

EWP foams at pH 7.0, with or without BC, were structured and kept their shape during manipulation. The overall structure and volume were stable for hours, as was shown from the results of the foam stability. Macroscopically, the aspect of EWP foams with BC did not differ from the well-known whipped egg whites (control), which were white, opaque, and homogeneous. SPI foams (with and without BC) were similar, but in a light beige color and sometimes larger bubbles appeared on the top. Microscopically (Fig. 6), the air bubbles were tightly packed, resulting in shapes close to polyhedra. Conversely, SPI foams flow even at pH 3.0 and their volume decreased over time, even in the presence of BC. SPI foams do not form structured alveoli or packed bubbles. Instead, the bubbles move freely in the continuous phase and quickly coalesce and burst. Both EWP and SPI foams have a wide range of bubble sizes. The presence of BC in the foam, shifts the bubble diameter distribution toward larger sizes. SPI foams show both smaller and much larger bubbles than EWP foams. It must be noted that bigger SPI bubbles were seen bursting while preparing the slides and throughout the microscopic observation, so the results are illustrative and not precise. Contrariwise, EWP foams were stiff and stable to the point where, after converting the diameter measurements into an equivalent sphere volume, the ratio between the total bubble volume with and without BC was 1.56, very close to the 1.6-fold increase observed for 4 % EWP foams in Fig. 3.

Considering that using BC particles of larger size improved the proteins' foam capacity (Fig. 4), the mechanism of action relies on the presence of large flakes, roughly mixed with the foam and/or in the plateau borders. If the fibers were smaller or better dispersed, they would be more likely to be evenly distributed in the liquid phase (the thin films of the lamellae) or adsorb evenly at the foam's liquid-air interface. As observed experimentally (Table 1, Fig. 4), this was not the case. As mentioned in the introduction, it is known that particles can stabilize foams. These particles must have a suitable size, shape and contact angle at the liquid-air interface, acting mainly by reducing the water drainage due to gravitational forces. The presence of particles may also help stabilize the foam by other means, such as reducing disproportionation. In polyhedric foams, the lamellae are thin films commonly with a thickness of tenths of nm (Dickinson, 2010). In the current case, as seen in Fig. 6, the average distance between bubbles is in the range of tenths of micrometers, even though some bubbles are close together and

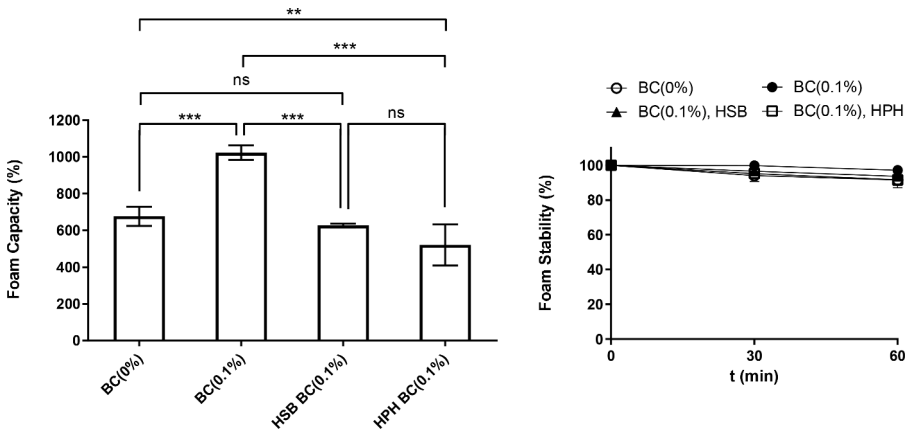

Fig. 4. Effect of 0.1 % BC size on the (left side) FC and (right side) FS of 4 % EWP with addition of 0.1 % of BC wet-ground to different extents, at pH 7.0. Datasets were compared with each other using one-way ANOVA followed by Tukey's Multiple Comparison Test (significant statistical differences at *** $p < 0.001$, **** $p < 0.0001$; ns - not significant).

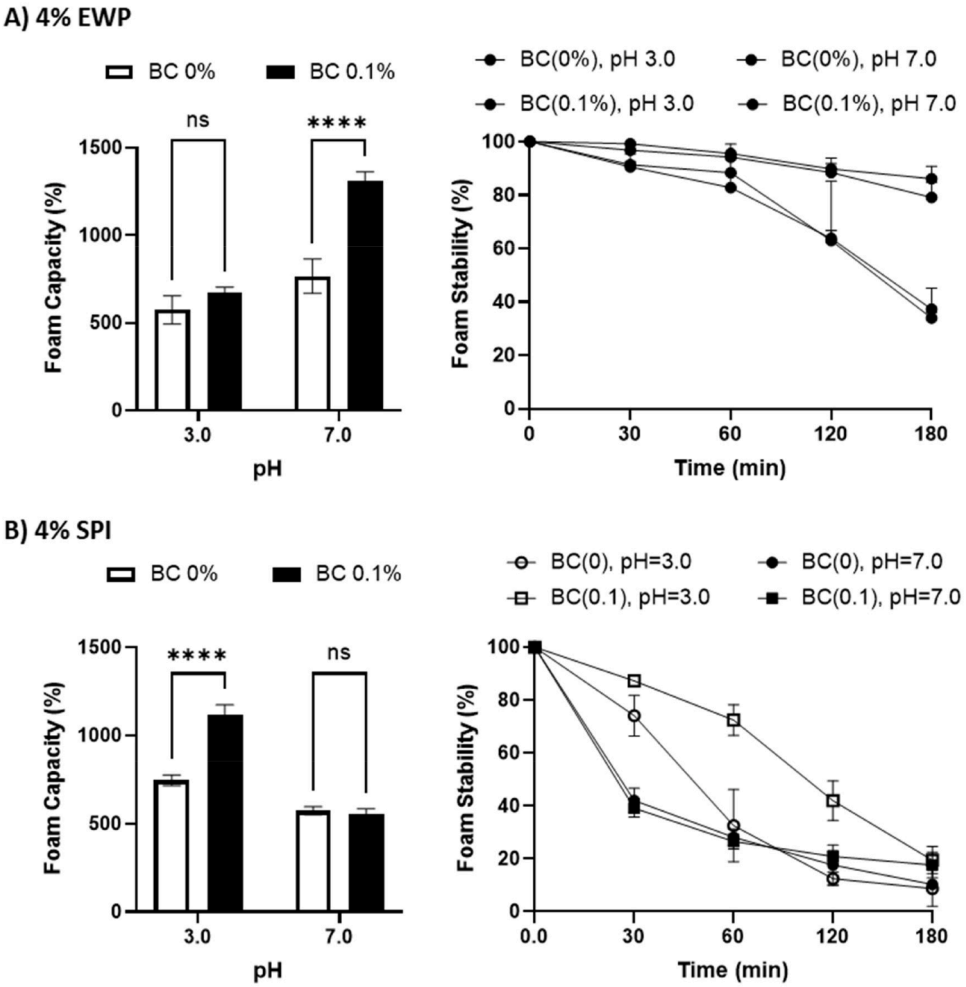

Fig. 5. Influence of pH and BC on the foam capacity (left side) and foam stability (right side): of A) 4 % EWP and B) 4 % SPI. Datasets were compared with each other using two-way ANOVA followed by Šídák's Multiple Comparison Test (significant statistical differences at **** $p < 0.0001$; ns – not significant).

have deformed from a spherical shape (especially in the foams containing EWP). This raises the question of where the BC bundles (which can be up to 1 mm long – Table 1) are located in the foam. The Plateau borders and the nodes (where the Plateau borders meet) offer more space than the lamellae. However, protein foams are better defined as spherical foams with a significant volume of liquid available, and thus maybe there are not many restrictions for the location of the BC fibers.

To answer these questions, the foams were observed under fluorescence microscopy, staining the proteins with rhodamine B (red) and BC with calcofluor (blue). Fig. 7 shows representative images, highlighting the uneven, random distribution of BC. As discussed previously, the bubbles in the EWP foam are more compact and present a polyhedric

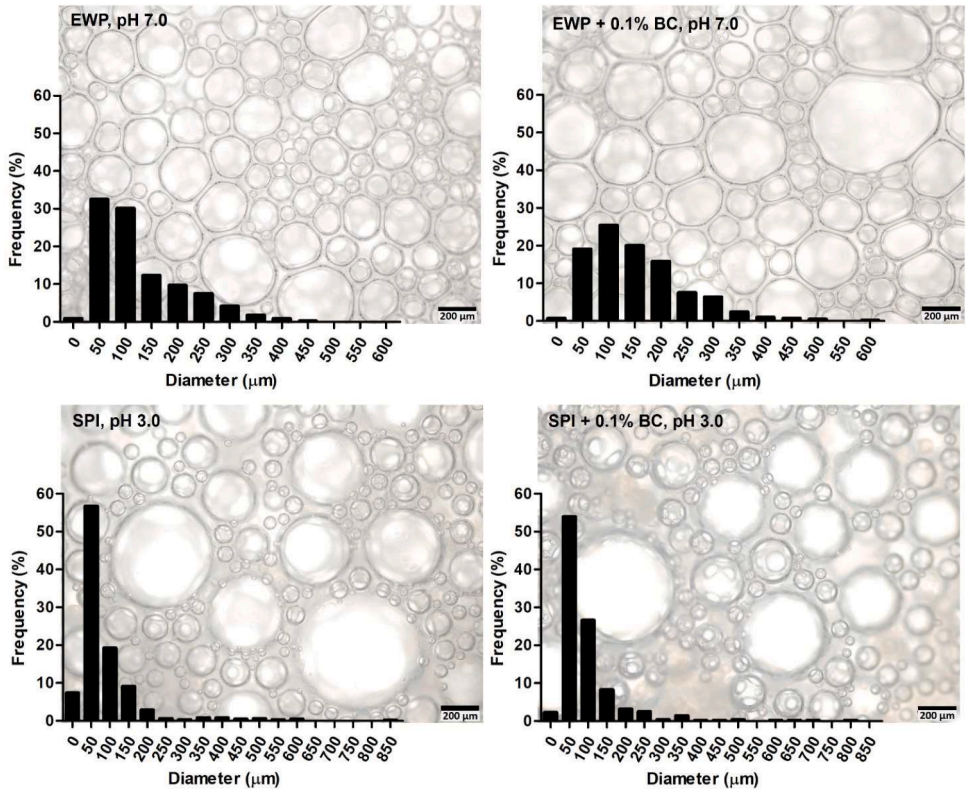

Fig. 6. Optical micrographs (40x magnification) of 4 % EWP foams at pH 7.0 and 4 % SPI foams at pH 3.0, with and without addition of 0.1 % BC). Inserts show the size distribution of the bubbles' diameters. Scale bar 200 μm.

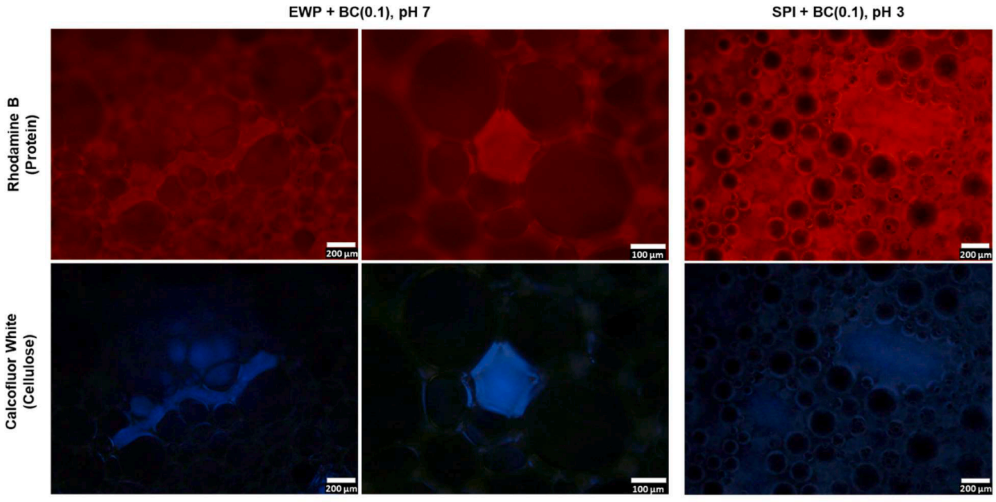

Fig. 7. Fluorescence microscopy images of 4 % EWP + 0.1 % BC foam at pH 7 (left) and SPI + 0.1 % BC foam at pH 3 (right), stained with Rhodamine B (protein, red) and Calcofluor White (BC, blue).

shape, while the bubbles in the SPI are round and move freely (Fig. 6). Some BC bundles have a size comparable to that of the bubbles, and others are much larger (Table 1 and Fig. 6). The effect of BC samples with different particle sizes suggests that indeed large flakes of BC are required to improve the proteins' foam capacity. It may be speculated that the presence of the large flakes stabilizes the bubbles as they are being generated by whipping, allowing a more effective foaming. Since the distribution of diameter sizes of the foam bubbles (Fig. 6) obtained with BC shifted to higher values (better seen for EWP), it may be concluded that the larger FC of BC-containing samples derives from greater air incorporation, translated in an increase in the size of individual bubbles. Fig. 7 shows that each bundle of BC is surrounded by several bubbles, as expected given its size. In some cases, some BC lumps in the liquid phase seem to surround a significant part of the bubbles. This interaction must be responsible for the higher FC. We believe that, during whipping, bubbles are being generated, but many are short lived. BC probably improves the stabilization of the bubbles, resulting in a higher FC. This hypothesis is supported by the observation noted above that BC seems to potentiate the FC capacity at the pH most favorable for each protein to generate a foam. While large agglomerates in solution exhibit a greater energy barrier for diffusion to the air-liquid interface during foam formation, BC is unlikely to play a surface-active role at the

interface.

We hypothesize that while air bubbles are being formed during protein whipping, the added BC will act as anchoring sites to which the newly formed bubbles (or existing ones) attach. Xiang *et al.* (Xiang et al., 2019) studied the generation and breakdown of aqueous foams stabilized by sodium dodecyl sulfate (SDS) in the presence of 0.3 % (m/m) cellulose nanofibrils (CNF). The CNF enhanced the viscosity and elasticity of both the continuous phase and the air/water interface. Initially, the foams with CNF- had higher liquid fractions, bigger bubbles, and were more stable. It was suggested that CNF formed aggregates in the Plateau borders and nodes of the foam, thus slowing down liquid drainage and bubble growth and improving FS. This mechanism potentially accounts for the observed improvement in the foam stability of EWP and SPI (noteworthy for 4 % SPI at pH 3.0 (Fig. 5B), and 4 % and 12 % EWP at pH 7.0 (Fig. 3), as seen by the reduction in drainage rate), which could be explained by the higher retention of liquid, avoiding its drainage, an effect favored by the BC high surface area and ability to absorb water. This effect – the ability of particles and aggregates to obstruct the junctions of the Plateau borders to slow down the liquid drainage, contributing to foam stabilization – has been reported by several authors (Asghari et al., 2016; Ellis et al., 2017; Gharbi & Labbafi, 2019; Jarpa-Parra et al., 2016). Interestingly, in our study, although an improvement in stability was recorded in the presence of BC (notwithstanding the significant impact on liquid drainage), a more remarkable impact was observed on the FC.

3.5. Rheological assessment

The viscosity and viscoelastic profile of the foams were assessed. The frequency dependence reveals how both viscous and elastic effects vary with the applied frequency. For both protein systems, the complex viscosity (Fig. 8) decreased with the increase in frequency. This is a characteristic of shear-thinning fluids (Bai et al., 2018), where at low frequencies the complex viscosity is high (more elastic) and decreases with increasing frequency, as elastic energy is converted to viscous energy. For SPI foams, a constant viscosity plateau was observed above 6 Hz, notably at pH 7.0 in the presence of BC. Overall, EWP foams have a significantly higher complex viscosity than SPI ones, which may explain the higher stability of EWP foams. Although the overall molecular weight of EWP is much lower than that of SPI, the complex viscosity of the foam seems to depend more on the tighter (for EWP) or looser (for SPI) alveolar structure than on structural features of the proteins. Regardless of the pH, BC at 0.1 % had no effect on the complex viscosity of EWP foams. In turn, higher FC at pH 7.0 leads to a better packed alveolar structure which results in a higher complex viscosity. For SPI, despite the significant improvement in the FC in the presence of BC at pH 3.0, a small reduction was observed in the complex viscosity. At pH 7.0, BC had no effect on FC, but it increased the complex viscosity. This effect could be expected, given the large size of BC bundles and their ability to absorb and drag water. This is unnoticed in the case of EWP probably because the tighter alveolar structure has a larger effect than BC itself.

The viscoelastic behavior of a system can be quantified by two components, the storage modulus (G') which describes the elastic response and the ability of a material to store energy; the loss modulus (G''), which measures the viscous component and provides information on the ability of a material to dissipate energy. From Fig. 9, for both protein foams, overall, the elastic behavior predominates over the viscous one (G' > G'') indicative of a solid-like consistency. For EWP at pH 7.0 (the conditions for higher foaming capacity), the viscoelastic profile is much superior to that at pH 3.0, with BC foams having a small reduction in the profiles comparatively to the control (Fig. 9a and b). Regarding this, it is worth reminding that EWP foams containing BC had larger bubbles, so there is more air in the same sample size. With a similar reduction effect of BC in the viscoelastic profile, SPI foams have higher profiles at pH 3.0 than those at pH 7.0 (Fig. 9c and d). Although BC had no effect in the FC and FS of SPI at pH 7.0 (Fig. 5), it significantly increased its elastic component (G'). Intriguingly, while both proteins present values of G' and G'' in the same order of magnitude at pH 3.0, the dispersions behave quite differently with an increase in pH to 7.0. Since each protein has a similar concentration at both pH values and both have a similar zeta potential at each pH, this effect is unexpected and deserves further study.

Overall, the addition of 0.1 % BC had little impact on the complex viscosity of the foams and caused only a small decrease in the viscoelastic moduli of EWP at pH 7.0 and SPI at pH 3.0, the same conditions where a greater amount of air was incorporated in the samples. In this way, it is expected that BC can be easily introduced into already well-known food foams, improving FC and water retention, without significantly altering their rheology or visual aspect.

4. Conclusions

This study investigated the effect of BC on the FC and FS of foams produced with EWP and SPI. The results demonstrated that BC can significantly increase the FC of EWP and SPI foams. Although BC influence on FS was minimal, it improved the liquid retention within the continuous phase of the foam. Also, BC may enhance the proteins' FC more effectively at each protein's optimal pH for foaming, but this effect is not due to a reduction in surface tension. Instead, it may be associated with its particle size, with larger BC flakes being more effective, possibly through a physical stabilization of the foam's structure upon whipping, where the BC flakes may act as anchoring points for the formed air

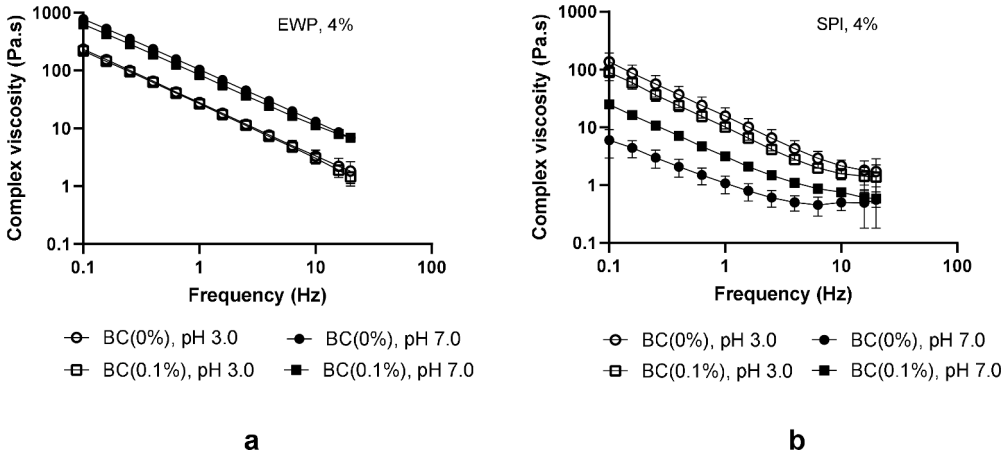

Fig. 8. Effect of bacterial nanocellulose (BC) and pH on the frequency dependent complex viscosity of (a) egg white protein (EWP) and (b) soy protein isolate (SPI), at 4 % (w/w).

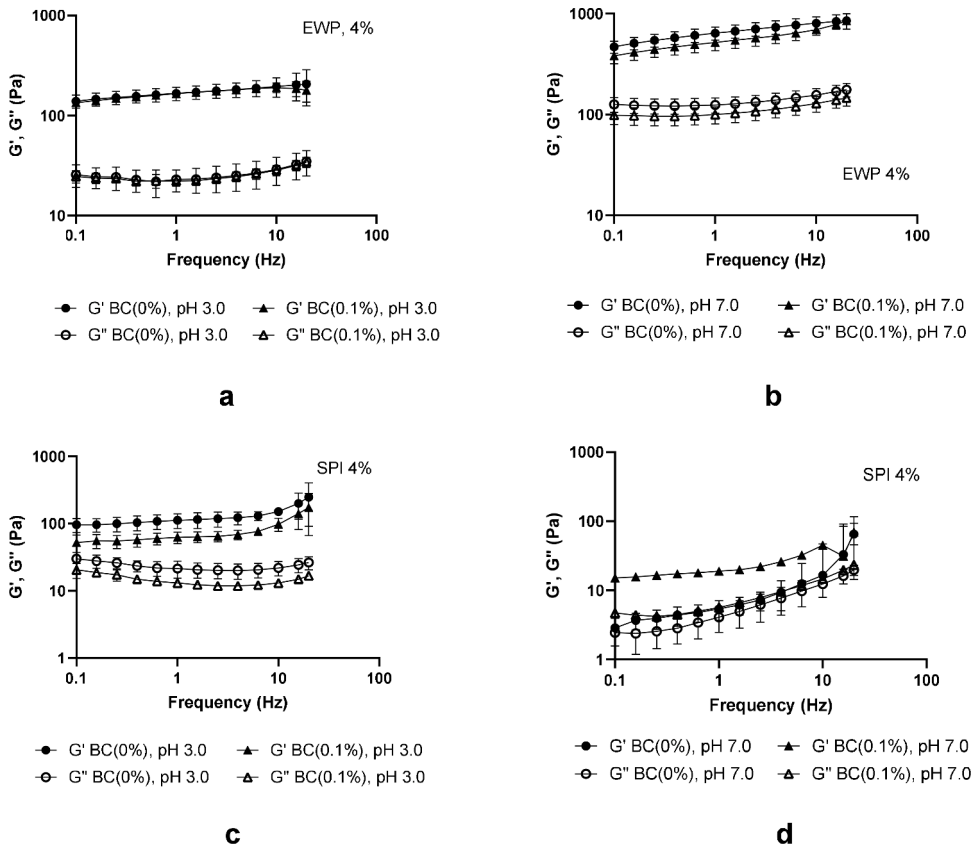

Fig. 9. Effect of bacterial nanocellulose (BC) and pH on the storage (G') and loss (G") moduli of (a, b) egg white protein (EWP) and soy protein isolate (SPI) (c, d), at 4 % (m/m).

bubbles. The viscoelastic profiles of the shear thinning foams confirmed that the elastic properties dominate, which correlates with the foams' stability and consistency.

Overall, this work underscores the potential of BC as a functional ingredient in the development of aqueous food foams, with implications for food texture and stability. Its use could be particularly advantageous in applications requiring high foam volume and structural integrity. Foam stabilization remains a complex and non-trivial subject. In future work, we will attempt to elucidate the unconventional BC foam-booster mechanisms of action. We will also explore the broader applicability of these findings in food technology - in different products such as ice-creams – addressing both the technological and the sensorial effects of BC.

CRediT authorship contribution statement

Daniela Martins: Writing – review & editing, Writing – original draft, Visualization, Validation, Methodology, Investigation, Formal analysis, Data curation. **Niloofar Khodamoradi:** Methodology, Investigation, Data curation. **Ricardo Silva-Carvalho:** Writing – review & editing, Investigation, Data curation. **Miguel Gama:** Writing – review & editing, Writing – original draft, Conceptualization. **Mehran Moradi:** Writing – review & editing, Methodology, Conceptualization. **Fernando Dourado:** Writing – review & editing, Visualization, Supervision, Formal analysis.

Declaration of competing interest

The authors declare that they have no known competing financial interests or personal relationships that could have appeared to influence the work reported in this paper.

Data availability

Data will be made available on request.

Acknowledgments

This study was supported by the Portuguese Foundation for Science and Technology (FCT) under the scope of the strategic funding of UIDB/04469/2020 unit, and by LABBELS – Associate Laboratory in Biotechnology, Bioengineering and Microelectromechanical Systems, LA/P/0029/2020.

References

Abeyrathne, E. D. N. S., Lee, H. Y., & Ahn, D. U. (2013). Egg white proteins and their potential use in food processing or as nutraceutical and pharmaceutical agents—A review. *Poultry Science, 92*(12), 3292–3299.

Alargova, R. G., et al. (2004). Foam Superstabilization by Polymer Microrods. *Langmuir : The ACS Journal of Surfaces and Colloids, 20*(24), 10371–10374.

Andrade, F. K., Pertile, et al. (2010). Bacterial cellulose: Properties, production and applications. *Cellulose: Structure and properties, derivatives and industrial uses* (pp. 427–458). New York, New York, USA: Nova Science Publishers. A. Lejeune and T. Deprez, Editors.

Asghari, A. K., et al. (2016). Interfacial and foaming characterisation of mixed protein-starch particle systems for food-foam applications. *Food Hydrocolloids, 53*, 311–319.

Azeredo, H. M., et al. (2019). Bacterial cellulose as a raw material for food and food packaging applications. *Frontiers in Sustainable Food Systems, 3*, 7.

Bai, L., et al. (2018). Adsorption and assembly of cellulosic and lignin colloids at oil/water interfaces. *Langmuir : The ACS Journal of Surfaces and Colloids, 35*(3), 571–588.

Barnes, G., & Gentle, L. (2011). *The gas-liquid interface: Adsorption; films and foams; aerosol, in interfacial science: An introduction* (p. 58). New York: Oxford University Press Inc.. G. Barnes and L. Gentle, Editors.

Bertsch, P., et al. (2019). Designing Cellulose Nanofibrils for Stabilization of Fluid Interfaces. *Biomacromolecules, 20*(12), 4574–4580.

Butt, H. J., Graf, K., & Kappl, M. (2003a). *Liquid surfaces, in physics and chemistry of interfaces* (pp. 4–25). Germany: Wiley-VCH Verlag GmbH & Co. KGaA.

Butt, H. J., Graf, K., & Kappl, M. (2003b). *Surfactants, micelles, emulsions, and foams, in physics and chemistry of interfaces* (pp. 246–279). Wiley-VCH Verlag GmbH & Co. H.-J. Butt, K. Graf, and M. Kappl, EditorsKGaA: Germany.
Capron, I., Rojas, O. J., & Bordes, R. (2017). Behavior of nanocelluloses at interfaces. *Current Opinion in Colloid & Interface Science, 29*, 83–95.
Cazón, P., & Vázquez, M. (2021). Bacterial cellulose as a biodegradable food packaging material: A review. *Food Hydrocolloids, 113*, Article 106530.
Cervin, N. T., et al. (2015). Mechanisms behind the stabilizing action of cellulose nanofibrils in wet-stable cellulose foams. *Biomacromolecules, 16*(3), 822–831.
Dabestani, M., & Yeganehzad, S. (2019). Effect of Persian gum and Xanthan gum on foaming properties and stability of pasteurized fresh egg white foam. *Food Hydrocolloids, 87*, 550–560.
de Amorim, J. D. P., et al. (2020). Plant and bacterial nanocellulose: Production, properties and applications in medicine, food, cosmetics, electronics and engineering. A review. *Environmental Chemistry Letters, 18*, 851–869.
Delahaije, R. J. B. M., et al. (2014). Quantitative description of the parameters affecting the adsorption behaviour of globular proteins. *Colloids and Surfaces B: Biointerfaces, 123*, 199–206.
Dickinson, E. (2010). Food emulsions and foams: Stabilization by particles. *Current Opinion in Colloid & Interface Science, 15*(1), 40–49.
Dickinson, E. (2017). Biopolymer-based particles as stabilizing agents for emulsions and foams. *Food Hydrocolloids, 68*, 219–231.
Dickinson, E. (2020). Advances in food emulsions and foams: Reflections on research in the neo-Pickering era. *Current Opinion in Food Science, 33*, 52–60.
Ding, L., et al. (2020). Changes in protein structure and physicochemical properties of egg white by super critical carbon dioxide treatment. *Journal of Food Engineering, 284*, Article 110076.
Ellis, A. L., et al. (2017). Stabilisation of foams by agar gel particles. *Food Hydrocolloids, 73*, 222–228.
Engelhardt, K., et al. (2013). pH effects on the molecular structure of beta-lactoglobulin modified air-water interfaces and its impact on foam rheology. *Langmuir : The ACS Journal of Surfaces and Colloids, 29*(37), 11646–11655.
Foegeding, E. A., Luck, P. J., & Davis, J. P. (2006). Factors determining the physical properties of protein foams. *Food Hydrocolloids, 20*(2), 284–292.
Gao, J., et al. (2022). Effects of guar gum or xanthan gum addition in conjunction with pasteurization on liquid egg white. *Food Chemistry, 383*, Article 132378.
Gharbi, N., & Labbafi, M. (2019). Influence of treatment-induced modification of egg white proteins on foaming properties. *Food Hydrocolloids, 90*, 72–81.
Gregory, D. A., et al. (2021). Bacterial cellulose: A smart biomaterial with diverse applications. *Materials Science and Engineering: R: Reports, 145*, Article 100623.
He, Z., et al. (2015). Foaming characteristics of commercial soy protein isolate as influenced by heat-induced aggregation. *International Journal of Food Properties, 18*(8), 1817–1828.
Hu, Z., et al. (2016). Stable Aqueous Foams from Cellulose Nanocrystals and Methyl Cellulose. *Biomacromolecules, 17*(12), 4095–4099.
Indrawati, L., et al. (2008). Effect of processing parameters on foam formation using a continuous system with a mechanical whipper. *Journal of Food Engineering, 88*(1), 65–74.
Jarpa-Parra, M., et al. (2016). Understanding the stability mechanisms of lentil legumin-like protein and polysaccharide foams. *Food Hydrocolloids, 61*, 903–913.
Jin, H., et al. (2022a). Ultrasonic-assisted spray drying as a tool for improving the instant properties of egg white powder. *Food Structure, 33*, Article 100289.
Jin, H., et al. (2022b). Adsorption kinetics of ovalbumin and lysozyme at the air-water interface and foam properties at neutral pH. *Food Hydrocolloids, 124*, Article 107352.
Jin, H., et al. (2023). Comprehensive identification and hydrophobic analysis of key proteins affecting foam capacity and stability during the evolution of egg white foam. *Food Hydrocolloids, 134*, Article 108033.
Kalashnikova, I., et al. (2011). New pickering emulsions stabilized by bacterial cellulose nanocrystals. *Langmuir : The ACS Journal of Surfaces and Colloids, 27*(12), 7471–7479.
Kalashnikova, I., et al. (2012). Modulation of cellulose nanocrystals amphiphilic properties to stabilize oil/water interface. *Biomacromolecules, 13*(1), 267–275.
Keshk, S. M. (2014). Bacterial cellulose production and its industrial applications. *Journal of Bioprocessing & Biotechniques, 4*(2), 150.
Kondo, T., Rytczak, P., & Bielecki, S. (2016). Chapter 4 - Bacterial nanocellulose characterization. *Bacterial nanocellulose* (pp. 59–71). Amsterdam: Elsevier. M. Gama, F. Dourado, and S. Bielecki, Editors.
Kuropatwa, M., Tolkach, A., & Kulozik, U. (2009). Impact of pH on the interactions between whey and egg white proteins as assessed by the foamability of their mixtures. *Food Hydrocolloids, 23*(8), 2174–2181.
Kutuzov, S., et al. (2007). On the kinetics of nanoparticle self-assembly at liquid/liquid interfaces. *Physical Chemistry Chemical Physics, 9*(48), 6351–6358.
Lam, S., Velikov, K. P., & Velev, O. D. (2014). Pickering stabilization of foams and emulsions with particles of biological origin. *Current Opinion in Colloid & Interface Science, 19*(5), 490–500.
Lee, K. Y., et al. (2014). More than meets the eye in bacterial cellulose: Biosynthesis, bioprocessing, and applications in advanced fiber composites. *Macromolecular Bioscience, 14*(1), 10–32.
Li, J., et al. (2022). Soy protein isolate: An overview on foaming properties and air–liquid interface. *International Journal of Food Science & Technology, 57*(1), 188–200.
Li, Q., et al. (2021a). Application of nanocellulose as particle stabilizer in food pickering emulsion: scope, merits and challenges. *Trends in Food Science & Technology, 110*, 573–583.
Li, T., et al. (2021b). Developing fibrillated cellulose as a sustainable technological material. *Nature, 590*(7844), 47–56.
Liu, Z., et al. (2021). Bacterial cellulose nanofibers improved the emulsifying capacity of soy protein isolate as a stabilizer for pickering high internal-phase emulsions. *Food Hydrocolloids, 112*, Article 106279.
Luo, Y., & Hu, Q. (2017). 7 - Food-derived biopolymers for nutrient delivery. *Nutrient delivery* (pp. 251–291). Academic Press. A.M. Grumezescu, Editor.
Ma, Z., et al. (2022). Inhibiting effect of dry heat on the heat-induced aggregation of egg white protein. *Food Chemistry, 387*, Article 132850.
Martins, D., et al. (2020a). Dry bacterial cellulose and carboxymethyl cellulose formulations with interfacial-active performance: Processing conditions and redispersion. *Cellulose, 27*(11), 6505–6520 (London, England).
Martins, D., et al. (2020b). A dry and fully dispersible bacterial cellulose formulation as a stabilizer for oil-in-water emulsions. *Carbohydrate Polymers, 230*, Article 115657.
Medronho, B., & Lindman, B. (2014). Competing forces during cellulose dissolution: From solvents to mechanisms. *Current Opinion in Colloid & Interface Science, 19*(1), 32–40.
Mohanan, A., Nickerson, M. T., & Ghosh, S. (2020). Utilization of pulse protein-xanthan gum complexes for foam stabilization: The effect of protein concentrate and isolate at various pH. *Food Chemistry, 316*, Article 126282.
Murray, B. S. (2020). Recent developments in food foams. *Current Opinion in Colloid & Interface Science, 50*, Article 101394.
Narsimhan, G., & Xiang, N. (2018). Role of proteins on formation, drainage, and stability of liquid food foams. *Annual Review of Food Science and Technology, 9*(1), 45–63.
Navya, P. V., et al. (2022). Bacterial cellulose: A promising biopolymer with interesting properties and applications. *Int J Biol Macromol, 220*, 435–461.
Oduse, K., et al. (2018). Electrostatic complexes of whey protein and pectin as foaming and emulsifying agents. *International Journal of Food Properties, 20*, 1–15.
Okiyama, A., Motoki, M., & Yamanaka, S. (1993). Bacterial cellulose IV. Application to processed foods. *Food Hydrocolloids, 6*(6), 503–511.
Paximada, P., et al. (2016). Effect of bacterial cellulose addition on physical properties of WPI emulsions. Comparison with common thickeners. *Food Hydrocolloids, 54*, 245–254.
Perumal, A. B., et al. (2022). Nanocellulose: Recent trends and applications in the food industry. *Food Hydrocolloids, 127*, Article 107484.
Pugh, R. J. (1996). Foaming, foam films, antifoaming and defoaming. *Advances in Colloid and Interface Science, 64*, 67–142.
Queirós, E. C., et al. (2021). Hemostatic dressings made of oxidized bacterial nanocellulose membranes. *Polysaccharides, 2*, 80–99. https://doi.org/10.3390/polysaccharides2010006
Razi, S. M., et al. (2022). An overview of the functional properties of egg white proteins and their application in the food industry. *Food Hydrocolloids*, Article 108183.
Shi, Z., et al. (2014). Utilization of bacterial cellulose in food. *Food Hydrocolloids, 35*, 539–545.
Song, B., & Springer, J. (1996). Determination of interfacial tension from the profile of a pendant drop using computer-aided image processing: 2. Experimental. *Journal of Colloid and Interface Science, 184*(1), 77–91.
Sullca Grimaldez, L., & Martínez, K. D. (2021). Concentration trend study on foaming properties for native soy protein isolate treated by ultrasound and heating. *Journal of Food Science and Technology, 58*(12), 4666–4673.
Sun, J., et al. (2022). Impact of saccharides on the foam properties of egg white: Correlation between rheological, interfacial properties and foam properties. *Food Hydrocolloids, 122*, Article 107088.
Tang, T., et al. (2021). Effects of incorporating different kinds of peptides on the foaming properties of egg white powder. *Innovative Food Science & Emerging Technologies, 72*, Article 102742.
Tang, T., et al. (2022). Effect of modified egg white powder on the properties of angel cakes. *Journal of Food Engineering, 326*, Article 111012.
Urade, R. (2011). Chapter 38 - Fortification of bread with soy proteins to normalize serum cholesterol and triacylglycerol levels. in. *Flour and breads and their fortification in health and disease prevention* (pp. 417–427). San Diego: Academic Press. V.R. Preedy, R.R. Watson, and V.B. Patel, Editors.
Wang, J., et al. (2022). Ovomucin may be the key protein involved in the early formation of egg-white thermal gel. *Food Chemistry, 366*, Article 130596.
Warnakulasuriya, S. N., & Nickerson, M. T. (2018). Review on plant protein–polysaccharide complex coacervation, and the functionality and applicability of formed complexes. *Journal of the Science of Food and Agriculture, 98*(15), 5559–5571.
Xia, W., et al. (2022). Selective proteolysis of β-conglycinin as a tool to increase air-water interface and foam stabilising properties of soy proteins. *Food Hydrocolloids, 130*, Article 107726.
Xiang, W., et al. (2019). How Cellulose Nanofibrils Affect Bulk, Surface, and Foam Properties of Anionic Surfactant Solutions. *Biomacromolecules, 20*(12), 4361–4369.
Xiao, N., et al. (2021). A review on recent advances of egg byproducts: Preparation, functional properties, biological activities and food applications. *Food Research International, 147*, Article 110563.
Zayas, J. F. (1997). *Foaming properties of proteins, in functionality of proteins in food* (pp. 260–309). Berlin, Heidelberg: Springer Berlin Heidelberg. J.F. Zayas, Editor.
Zhang, T., et al. (2022a). How does dextran sulfate promote the egg white protein to form transparent hydrogel? the gelation mechanism and molecular force changes. *Food Hydrocolloids, 133*, Article 107901.

Zhang, X., et al. (2020). Edible foam based on pickering effect of bacterial cellulose nanofibrils and soy protein isolates featuring interfacial network stabilization. *Food Hydrocolloids, 100*, Article 105440.
Zhang, X., et al. (2023). Utilization of ovalbumin-propylene glycol alginate complex system for superior foam: The effect of pH-driven phase behavior. *Food Hydrocolloids, 135*, Article 108169.
Zhang, Y., et al. (2022b). Recent development of egg protein fractions and individual proteins as encapsulant materials for delivery of bioactives. *Food Chemistry*, Article 134353.